IAEA Technical Committee Meeting on Research Using Small Tokamaks
Würzburg, 28 - 29 September 1992

Hard X-ray Intensity Reduction during Lower Hybrid Current Drive Experiments

J. Mlynář
Faculty of Math. and Physics, Charles University, Prague
J. Stöckel, P. Magula
Institute of Plasma Physics, Prague

Abstract

A strong reduction of monitored hard X-ray intensity is observed during lower hybrid current drive (LHCD) at the Castor tokamak. We interpret it as an improvement of the runaway electron confinement. This supposition is reinforced by observation of a decrease of magnetic fluctuations level during LHCD phase of the discharge.

Hard X-ray Intensity Reduction during Lower Hybrid Current Drive Experiments

J. Mlynář[1], J. Stöckel, P. Magula
Institute of Plasma Physics CSAS
Za Slovankou 3, 182 11 PRAGUE 8

1 Introduction

In case that some changes in global hard X-ray emission were observed during a tokamak shot, runaway electrons behaviour is to be studied. The hard X-rays are produced mainly as high-energy runaway electrons bremsstrahlung in the limiter or in the walls. If global plasma instabilities can be excluded, the observed process has to be attributed to changes either in runaway electrons production rate or in runaway electrons cross-field transport. The production rate rises with a rising electric field and/or with a rising plasma density (see [1]), while the cross-field transport rises with rising electric field (i.e. the outward shift of the runaway electron drift orbit rises, see [1]) and/or with rising magnetic fluctuations level [2].

Let us briefly describe the connection between fluctuations and a test electron cross-field transport. Assume the perpendicular velocity of the tokamak plasma particles is derived from drifts in the poloidal electrostatic and radial magnetic fluctuations:

$$v_\perp = \frac{\tilde{E}}{B_o} + v_\| \frac{\tilde{B}}{B_o}$$

Hence, significance of the magnetic fluctuations in the cross-field transport increases with the parallel velocity. A coefficient of a radial diffusion of the test particle can be defined by random-walks as follows:

$$D = \frac{(\Delta r)^2}{2\tau} = \pi R \frac{v_\perp^2}{v_\|}$$

where $\Delta r = v_\perp \tau$ is the average radial shift during one revolution round the torus $\tau = (2\pi R)/v_\|$. Herefrom, the resulting diffusion coefficient is:

$$D = \pi R \left[\frac{1}{v_\|} \left(\frac{\tilde{E}}{B_o} \right)^2 + v_\| \left(\frac{\tilde{B}}{B_o} \right)^2 \right]$$

as the mixed term $\sim \tilde{E} \cdot \tilde{B}$ is zero according to the assumptions.

The significance of the two terms in case of the Castor tokamak ($\tilde{E} \doteq 1000\, V/m, \tilde{B} \doteq 22\, \mu T$) is demonstrated in fig. 1 . Herefrom it follows that the electrostatic fluctuations play a dominant role for the cross-field transport of thermal electrons ($E \leq 400\, eV$), while the magnetic fluctuations are significant for the cross-field transport of high-energy runaway electrons which are responsible for the hard X-ray production ($E \geq 100\, keV$).

---

[1] Ph.D. student of Faculty of Math. and Physics, Charles University, Prague

2 Experimental Setup

The Castor tokamak is a small tokamak with major and minor plasma radii $R = 0.4\,m$ and $a = 0.085\,m$ respectively. Hydrogen plasma at a quasistationary density $n \doteq 6{\cdot}10^{18}\,m^{-3}$ is confined in a toroidal magnetic field $B_T \doteq 1\,T$ and carries current $I_P \doteq 12\,kA$. Wave-plasma interaction at lower hybrid frequency is studied at this tokamak. The RF power ($P_{RF} < 40\,kW, f = 1.25\,\mathrm{GHz}$) can be launched into the plasma via a three waveguide multijunction grill (phaseshift $\phi = 90^0$ between adjacent wavequides).

The hard X-ray monitor is situated outside the vacuum vessel approximately 2 metres above the tokamak limiter. We use an unshielded $\o 40 \times 30\,mm$ NaI(Tl) scintilator on a simple photomultiplier, its energy range is approx. $50\,keV - 1.5\,MeV$. In fact, outside the Castor tokamak vessel hard X-rays can be detected in the range approx. from $100\,keV$ (lower energies are largely absorbed in vessel materials) to $500\,keV$ (the runaway electrons energy limit) [3].

A set of coils which determine the magnetic field characteristics is located on a poloidal ring within the scrape-off layer of the tokamak. The poloidal symmetry of the magnetic fluctuations level was experimentally proved in [4], therefore signal from just one of the coils may represent the fluctuation measurements. It is proceeded in an analog correlator so that a mean square value $\langle \tilde{B}^2 \rangle$ of the signal is studied.

3 Results

A typical evolution of a LHCD shot (full line) as compared to purely Ohmic shot (dashed line) is shown in fig. 2(a). The relative drop of the loop voltage observed during the LHCD application (from the $15th$ to the $20th\,ms$) is connected with the noninductive current generation (total plasma current is constant). Simultaneously, less H_α intensity and a higher plasma density is observed during LHCD (see fig. 2(a)). Herefrom, an improvement of the global particle confinement time during LHCD follows [5].

A strong reduction of monitored hard X-ray intensity is observed during the lower hybrid current drive phase of the discharge.

Some connection between the loop voltage drop and the hard X-ray reduction is to be expected as the loop voltage obviously influences rate, energy and cross-field transport of runaway electrons which produce the hard X-rays. Therefore we studied the loop voltage drop and the hard X-ray reduction versus the RF power level as well as the relation between the two signal reductions in detail; the relative reduction of the signals was considered (see figure captions). Time interval where the plasma density changes are negligible was elaborated so that the influence of the density changes to the runaway electrons production needn't be examined.

Results are summarized in figs. 3 and 4. We found that the hard X-rays intensity falls after the RF switch on much deeper than the loop voltage does (see fig. 3). Next, we found a time-independent relation between the hard X-rays and the loop voltage reductions, see fig. 4.

A substantial decrease of runaway electrons production during the loop voltage drop is the most trivial interpretation of the observed phenomenon. However, this idea cannot explain why the hard X-ray intensity signal falls down suddenly with the LHCD switch on (the high energy runaway electrons acceleration time on the Castor tokamak is in order of one millisecond [3]). Therefore, we suppose that an improvement of the runaway electrons confinement is observed.

As we mentioned in the introduction, an improvement of runaway electron confinement may be interpreted as a consequence of:

1. Substantially slower outward shift of the runaway electrons orbits due to less curvature drift acceleration during the loop voltage decrease;
2. Less cross-field diffusion of runaway electrons due to a reduction of magnetic fluctuations during LHCD.

In the above described shots the loop voltage is far away from being zero during LHCD phase, while hard X-ray radiation almost vanishes (see figs. 2 and 3). Herefrom, one can deduce that the first interpretation cannot fully explain the observed phenomena.

To prove directly the importance of the second possibility we decided to measure the magnetic fluctuations next. By a good luck this could be realised in a discharge regime with no loop voltage reduction during LHCD phase (see fig. 2(b)). Consequently, there is no observable current drive in this regime, though the characteristics of the target plasma (namely the plasma density) are very similar to the first discussed measurements, see fig. 2, dashed lines[2].

Though the loop voltage drop was not observed, the hard X-rays were reduced during LHCD again, see fig 2(b). Hence, the effects of LHCD application on hard X-rays signal cannot be definitely caused by the loop voltage drop alone.

As expected, a doubtless reduction of magnetic fluctuations was observed during LHCD, see fig. 2(b). This reduction corresponds to the reduction of hard X-rays, though it is not so deep; both of them increase with the RF power, see fig. 5. The connection between the reduction of magnetic fluctuations and the reduction of hard X-rays does not hold any dependence on time (which means the reductions are correlated) and it seems to be strongly nonlinear, see fig. 6.

In fact, this time the reduction was not so extensive as in the first discussed measurements, which may prove that the loop voltage decrease played some role in the hard X-rays reduction there. Moreover, this time the hard X-ray intensity reincreases sooner (within the interval of LHCD application), but this effect can be easily explained by the larger radial position shift of the plasma column (compare hard X-ray signals in fig. 2(a) and in fig. 2(b) and the corresponding radial plasma position).

No transport code for modelling the connection between magnetic fluctuations and hard X-ray production was applied so far at the Castor tokamak, as both the runaway electron diffusion and the hard X-ray production in the material are complex. Therefore, only qualitative discussions on empirical functions are worthwhile so far.

Let us still mention that a connection between runaway electrons confinement and thermal particles confinement was studied experimentally in [6].

4 Summary

A strong hard X-ray intensity reduction during a standard LHCD at the Castor tokamak was studied. From discussions it followed that the magnetic fluctuations level decrease is likely to be responsible for this effect beside the loop voltage decrease. To verify this idea, the connection between the magnetic fluctuation level and the hard X-ray intensity was studied in a nonstandard LHCD regime with a zero loop voltage reduction. These measurements strongly supported the

---

[2] In fact, the cause of the nonstandard LHCD effects in this regime is not fully clear. Probably a higher Z_{eff} is the cause, but an inappropriate plasma column position with respect to the mouth of the multijunction grill could do that as well. Moreover, this regime was found to be stable only for lower RF power ($P_{RF} < 20\,kW$) and a significant outwards plasma column shift occurs soon after the LHCD switch on.

concept that magnetic fluctuations level substantially influences the runaway electrons cross-field transport. Though, more data and a good code for modelling the anomalous transport and hard X-rays production would be of high value. Similar measurements especially for higher RF power should be carried out soon. Besides, the reduction of hard X-rays was observed in the experiments with edge plasma polarization lately; therefore, the magnetic fluctuations level in these experiments should be studied soon.

Acknowledgements:

The work was performed under CSAV grant No. 14310 and supported by IAEA contract No. 6702/RB.

References

[1] Knoepfel H., Spong D. A. : *Runaway Electrons in Toroidal Discharges*, Nucl. Fus. 19 (1979) 785

[2] Wooton, A.: Invited Lecture on the 19th EPS Conference on Contr. Fus. and Plasma Physics, Innsbruck, July 1992

[3] Mlynář J.: *The Hard X-Rays Analyses at the Castor Tokamak*, (in Czech), thesis, Charles University, Fac. of Math. and Physics, Prague 1991

[4] Valovič M. : *Suppression of Magnetic Fluctuations by Lower Hybrid Current Drive on the Castor Tokamak*, Cs. Institute of Plasma Phys. Rep. IPPCZ 300 (May 1990)

[5] Žáček F. et al. : *Fluctuation Studies on CASTOR and ASDEX Tokamaks during Lower Hybrid Current Drive*, IAEA TCM on Research Using Small Tokamaks, Oct 1991, Hefei, China

[6] Kwon O.J. et al. : *A Study of Runaway Electron Confinement in the Asdex Tokamak*, Nucl. Fus. 28 (1988) 1931

Figure Captions:

Fig. 1: Significance of the electrostatic and the magnetic fluctuations level to the test electron diffusion coefficient versus electron energy at the Castor tokamak ($\tilde{E} \doteq 1000\,V/m, \tilde{B} \doteq 22\,\mu T$), see introduction.

Fig. 2: Characteristic evolution of the tokamak Castor shots. Dashed line - purely Ohmic heating of the plasma (RF off); full line - lower hybrid current drive at the RF power of 20 kW applied from the 15th to the 20th millisecond of the shot.

Fig. 3: Relative reductions of the loop voltage and hard X-ray intensity vs. RF power at 1.5 ms after RF switch on. **Notice:**

- By the relative reduction we mean how much of the signal is lost as compared to a comparable purely Ohmic shot:

$$\text{relative reduction of } A \text{ in } \% = \frac{A_{OH} - A_{RF}}{A_{OH}} \cdot 100\ \%$$

- Data for this and the next figure were gathered from the Castor shots No. 2419-2430..

Fig. 4: Relative reduction of the hard X-ray intensity vs. relative reduction of the loop voltage. This dependence was within experimental errors found to be time-independent and only a very weak dependence on the RF power was observed.

Fig. 5: Relative reductions of the magnetic fluctuations level and hard X-ray intensity vs. RF power at 1.5 ms after RF switch on. **Notice:**

- Data for this and the next figure were gathered from the Castor shots No. 3155-3171.

Fig. 6: Relative reduction of the hard X-ray intensity vs. relative reduction of the magnetic fluctuations level. The same comment as in fig.4 is valid.

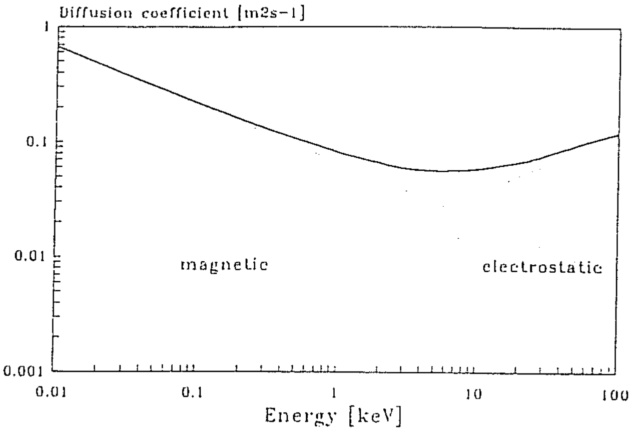
Diffusion coefficient [m2s-1]
1
0.1
0.01
0.001
magnetic
electrostatic
0.01
0.1
1
10
100
Energy [keV]

Fig. 1

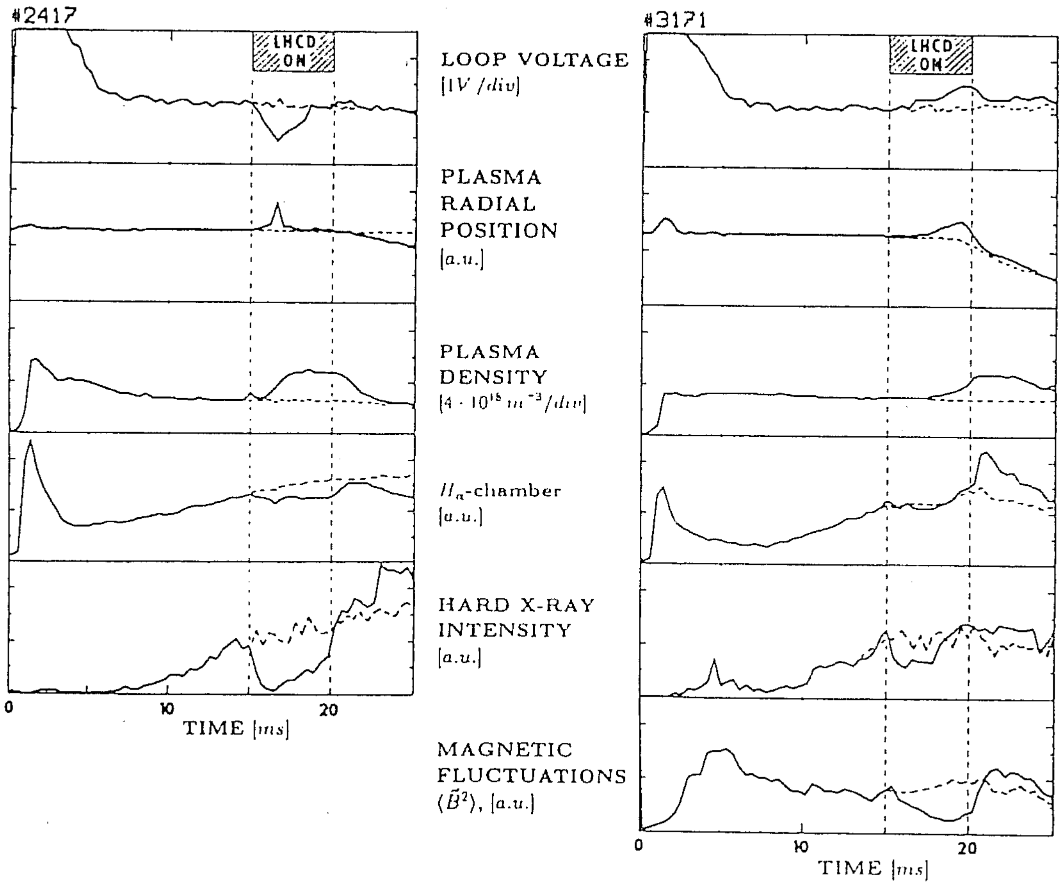
#2417
#3171
LHCD ON
LHCD ON
LOOP VOLTAGE
[1V/div]
PLASMA
RADIAL
POSITION
[a.u.]
PLASMA
DENSITY
[4 · 10^18 m^-3/div]
H_α-chamber
[a.u.]
HARD X-RAY
INTENSITY
[a.u.]
MAGNETIC
FLUCTUATIONS
$\langle \tilde{B}^2 \rangle$, [a.u.]
0
10
20
TIME [ms]
0
10
20
TIME [ms]

a

Fig. 2

b

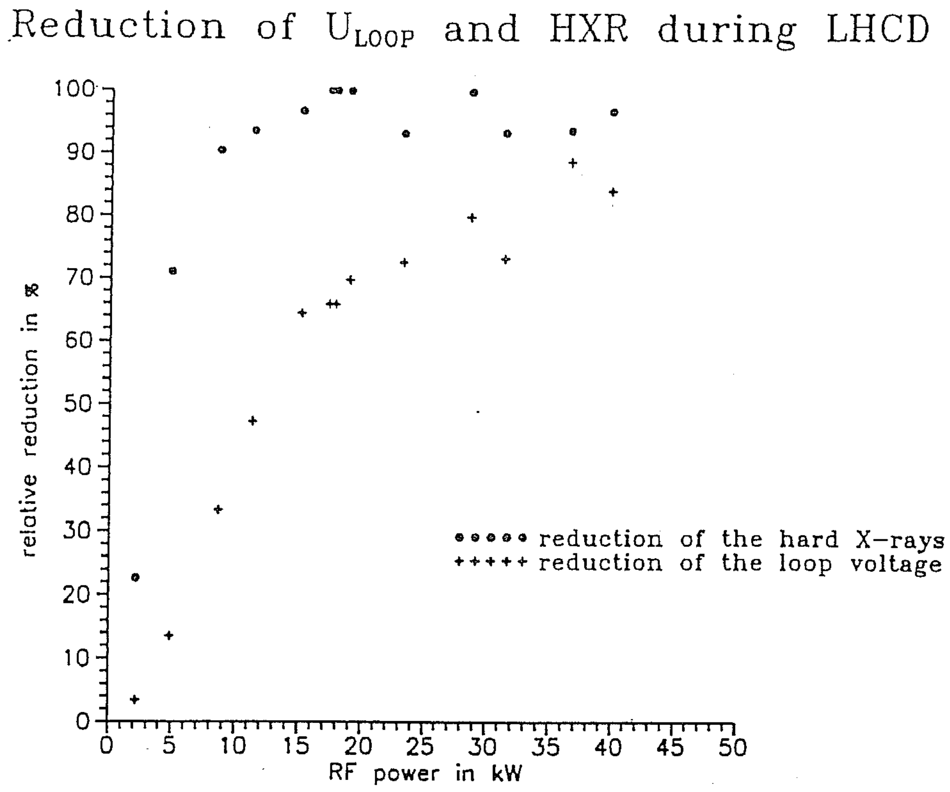
Reduction of U_{LOOP} and HXR during LHCD
relative reduction in %
0
10
20
30
40
50
60
70
80
90
100
RF power in kW
0
5
10
15
20
25
30
35
40
45
50
ooooo reduction of the hard X-rays
+++++ reduction of the loop voltage

Fig.3

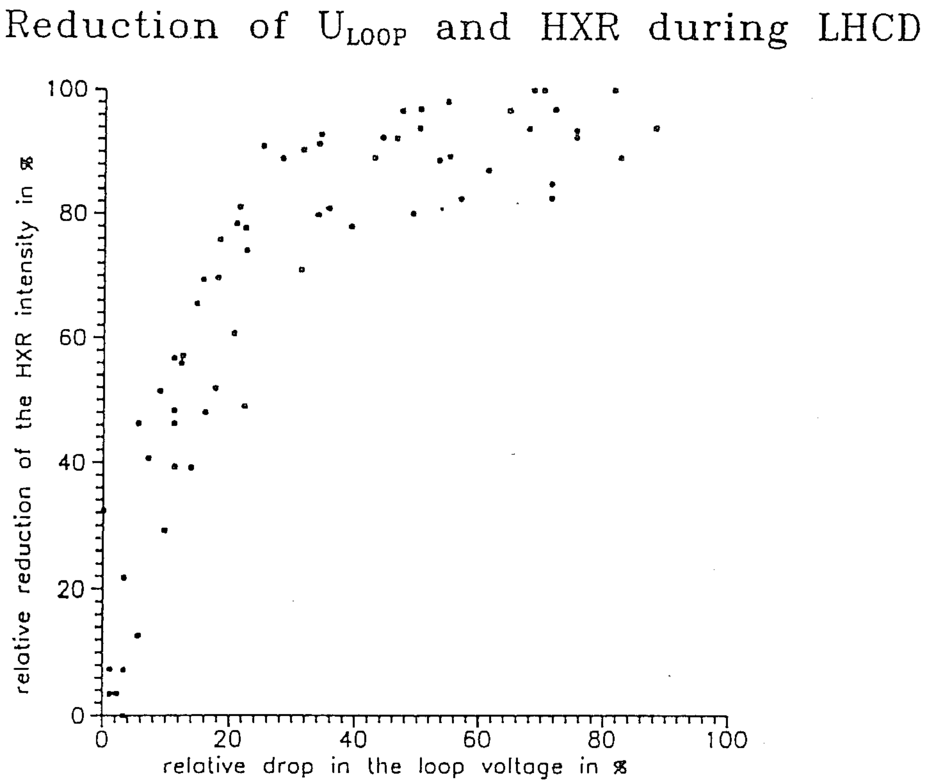
Reduction of U_{LOOP} and HXR during LHCD
relative reduction of the HXR intensity in %
0
20
40
60
80
100
relative drop in the loop voltage in %
0
20
40
60
80
100

Fig.4

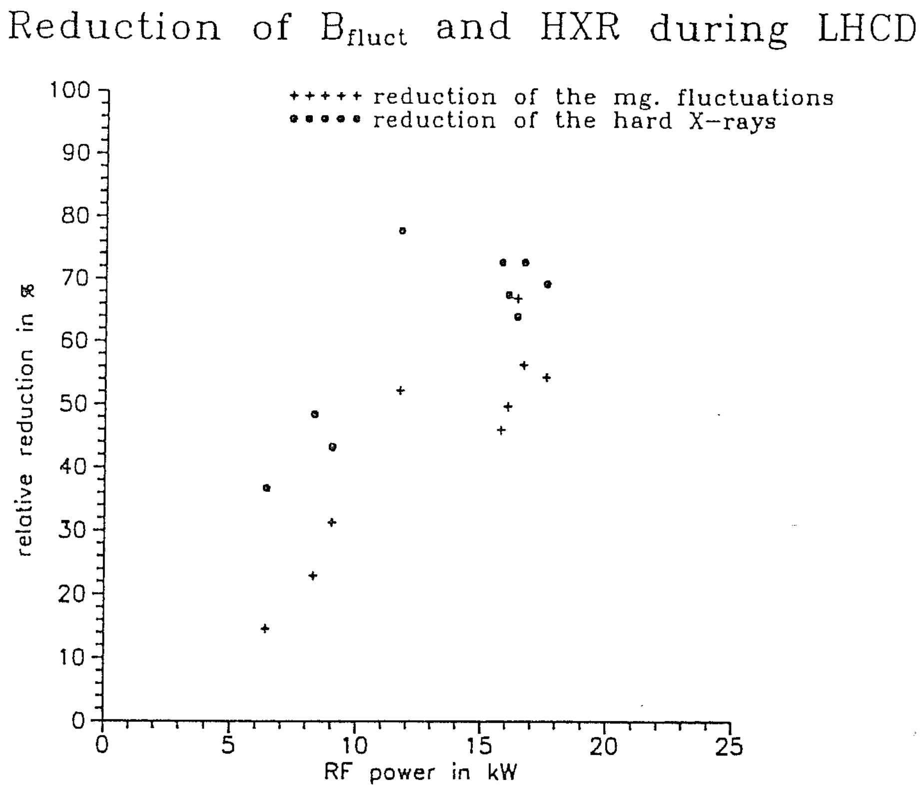
Reduction of B_{fluct} and HXR during LHCD
+++++ reduction of the mg. fluctuations
●●●●● reduction of the hard X-rays
relative reduction in %
RF power in kW
0
10
20
30
40
50
60
70
80
90
100
0
5
10
15
20
25

Fig.5

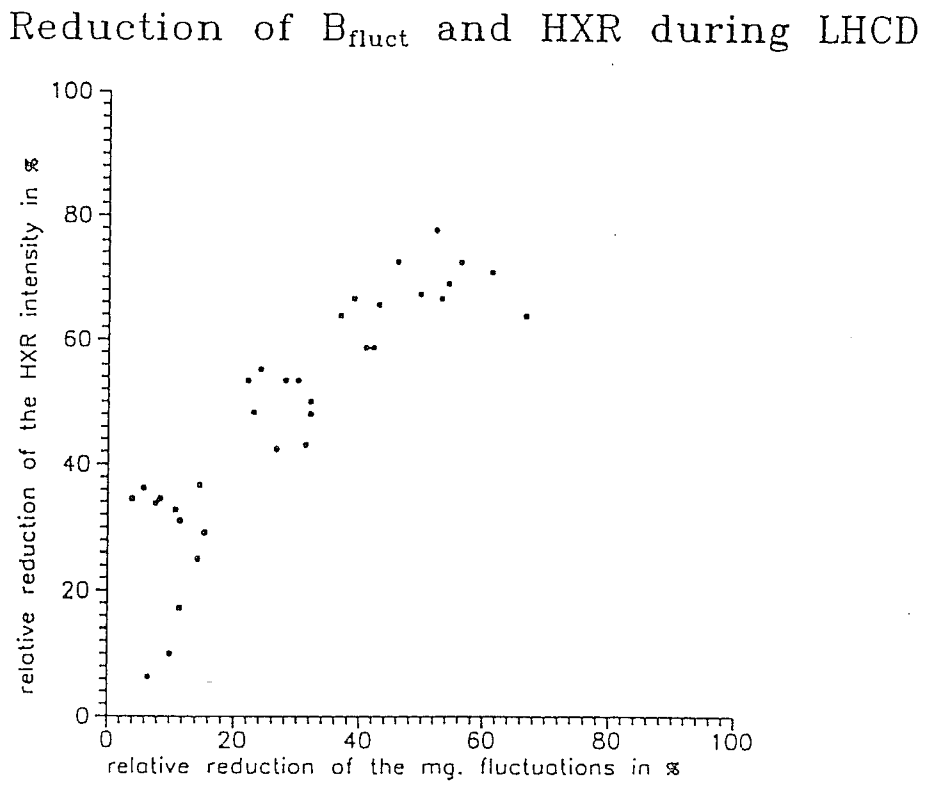
Reduction of B_{fluct} and HXR during LHCD
relative reduction of the HXR intensity in %
relative reduction of the mg. fluctuations in %
0
20
40
60
80
100
0
20
40
60
80
100

Fig.6